

Article

Evaluation and Comparison of Extremal Hypothesis-Based Regime Methods

Ishwar Joshi ¹ , Wenhong Dai ^{1,2,3,*}, Ahmed Bilal ¹ , Akhanda Raj Upreti ⁴ and Ziming He ¹

¹ College of Water Conservancy and Hydropower Engineering, Hohai University, Nanjing 210098, China; joshi@hhu.edu.cn (I.J.); ahmed.bilal@hhu.edu.cn (A.B.); heziming913@126.com (Z.H.)

² State Key Laboratory of Hydrology-Water Resources and Hydraulic Engineering, Nanjing 210098, China

³ National Engineering Research Center for Water Resources Efficient Utilization and Engineering Safety, Nanjing 210098, China

⁴ Key Laboratory of Integrated Regulation and Resource Development of Shallow Lakes, Ministry of Education, College of Environment, Hohai University, Nanjing 210098, China; akhandaraj@outlook.com

* Correspondence: wdai@hhu.edu.cn; Tel.: +86-13451891670

Received: 18 January 2018; Accepted: 19 February 2018; Published: 4 March 2018

Abstract: Regime channels are important for stable canal design and to determine river response to environmental changes, e.g., due to the construction of a dam, land use change, and climate shifts. A plethora of methods is available describing the hydraulic geometry of alluvial rivers in the regime. However, comparison of these methods using the same set of data seems lacking. In this study, we evaluate and compare four different extremal hypothesis-based regime methods, namely minimization of Froude number (MFN), maximum entropy and minimum energy dissipation rate (ME and MEDR), maximum flow efficiency (MFE), and Millar's method, by dividing regime channel data into sand and gravel beds. The results show that for sand bed channels MFN gives a very high accuracy of prediction for regime channel width and depth. For gravel bed channels we find that MFN and 'ME and MEDR' give a very high accuracy of prediction for width and depth. Therefore the notion that extremal hypotheses which do not contain bank stability criteria are inappropriate for use is shown false as both MFN and 'ME and MEDR' lack bank stability criteria. Also, we find that bank vegetation has significant influence in the prediction of hydraulic geometry by MFN and 'ME and MEDR'.

Keywords: hydraulic geometry; extremal hypothesis; bank strength; regime channels

1. Introduction

An alluvial channel, either artificial or natural, persists to deform its boundary by itself while transporting water and sediments. Nevertheless, if water and sediment rate remain constant, the deformation ceases after a certain period to achieve regime state or dynamic equilibrium or quasi-equilibrium [1]. In regime state, the hydraulic geometry characteristics of the channel remain invariant with time, thus having many economic and ecological benefits. Regime channels have been used for stable canal design [2,3] and to determine river response to environmental changes like climate shifts, construction of dams, land use changes, and river training [4–7].

A plethora of methods is available describing the hydraulic geometry of alluvial rivers in the regime. American Society of Civil Engineers (ASCE) Task Committee [8] has grouped regime methods into empirical (regime theory and power law), rational, or mechanistic and extremal hypotheses. Review of regime methods can be found in [9–13]. There is progressive development in the methods where old regime methods act as stepping stones for new methods which try to define dominant physical processes forming the regime channels. For example, in the development of empirical methods, Kennedy [14] was the first to observe that stable canals, neither aggrading nor degrading, exhibited

power-law relations between velocity and depth. Subsequently, Lacey [15] incorporated boundary materials in Kennedy's relations, while Blench [16] further developed Lacey's method by defining separate factors describing bed and bank composition. While previous empirical regime equations were only for sand bed channels, Hey and Thorne [2] and Davidson and Hey [17] extended regime equations to gravel bed channels. Similarly, in rational methods, Lane [18] gave the tractive force approach to predict regime channels but could not explain sediment transport in the channel. This deficiency was solved by Parker [19,20] by postulating lateral diffusion of suspended sediment and then used single perturbation techniques to calculate regime channel characteristics. Ikeda et al. [21] modified Parker's model for heterogeneous materials and Ikeda and Izumi [22] for vegetation influence.

Empirical regime methods have many drawbacks in that they are site-specific and dimensionally inhomogeneous [8]. Therefore, their validity is constrained to basins and data where they are developed. Farias et al. [23] have shown that regime methods based on extremal hypotheses predict regime channels better than empirical methods. Similarly, rational methods also have many drawbacks, for example, only regime channel depth can be readily determined from Parker's model, which yields larger depth for smaller channels and smaller depth for larger channels. Moreover, Nanson and Huang [13] argued that rational regime models can only be used for stable profiles at an individual cross-section of a channel. Of late, Khodashenas [24] found that rational methods did not give satisfactory results in predicting regime channels and proposed an additional study of these methods.

Although extremal methods have been called the illusion of progress [25], they have been used for stable canal design and to determine channel pattern [26], river response to land use changes, and channel changes [4], and to predict the equilibrium geometry of a river [27]. However, which extremal hypothesis should be used remains a topic of debate because there is no convincing theoretical explanation for any of the hypotheses [13,28].

Extremal methods or optimality theory is based on the assumption that regime state is achieved when a certain energy or mechanistically related parameter, K_* , is either maximized or minimized [1]. Generally regime channel characteristics B_R , h_R and S_R are determined by simultaneously solving the following three equations [1]:

$$Q = f_Q(B_R, h_R, S_R, c_R) \text{ (Resistance equation)} \quad (1)$$

$$Q_s = f_Q(B_R, h_R, S_R, c_R) \text{ (Bed load transport equation)} \quad (2)$$

$$dK_* = 0 \text{ (Optimization criteria)} \quad (3)$$

where Q is the bankfull discharge, B_R is the regime channel width, h_R is the regime channel depth, S_R is the regime channel slope, Q_s is the bed load, and c_R is the Chézy resistance coefficient at regime state defined by $c_R = f_c(h_R, S_R)$. Based on the parameter of optimization K_* the following extremal methods are found in the literature: maximum sediment transport capacity (MSTC) [29–31], minimum stream power (MSP) [26,32], minimum energy dissipation rate (MEDR) [33], minimum unit stream power (MUSP) [34], maximum friction factor (MFF) [35], and maximum flow efficiency (MFE) [27,28,36,37].

Though developed by different researchers, some of these methods tend to be equivalent. For example, MSP and MSTC give identical results [28,38]. MFE is the general case of MSP and MSTC [15,27,28]. MEDR is the general case of MSP and MUSP [35]. Davies and Sutherland [35] have shown that under certain circumstances, MFF is the general case of MEDR, MSP, and MUSP. In our study we have taken MFE as a typical representative of these methods because it has been widely used for regime channel computation [27] and to determine river channel pattern [13]. Moreover, MFE has been proven using the principle of least action [28].

In other developments, MSTC, MSP, MEDR, MUSP, MFF, and MFE have been criticised by Millar and Quick [38], Eaton and Millar [39], and Millar [40] for predicting very low regime channel width/depth ratios and thus resulting low values for regime channel width B_R and high values for depth h_R . For example, MFE yields a width/depth ratio of 2.5 while MEDR yields 2 [40]. This low prediction of width/depth ratio has been attributed to lack of bank stability or bank strength criteria

in their formulation [38–40]. Millar and Quick [38] thus developed a model which incorporated bank stability criteria in the model of MSTC which has the form

$$Q = f_Q(B_R, h_R, S_R, c_R) \text{ (Resistance equation)} \quad (4)$$

$$Q_s = f_Q(B_R, h_R, S_R, c_R) \text{ (Bed load transport equation)} \quad (5)$$

$$dK_* = 0 \text{ (Optimization criteria)} \quad (6)$$

$$\tau_{\text{bank}} \leq \tau_{\text{bankc}} \text{ (Bank stability criteria)} \quad (7)$$

where τ_{bank} is the shear stress of the bank, and τ_{bankc} is the critical shear stress of the bank. Eaton and Millar [39], using the model of Millar and Quick [38], have shown that regime models that are not constrained by bank stability are only suitable for highly resistant boundaries. Millar [40] again refined the model of Millar and Quick [38] with a different sediment transport equation and dimensionless form of MSTC. The model developed by Millar [40] is named as Millar's method for this article.

In contrast to MSTC, MSP, MEDR, MUSP, MFF, and MFE, minimization of Froude number (MFN) uses a width equation instead of a sediment transport equation. Yalin and Da Silva [1] contend that the value of bed load Q_s in Equation (2) is not known beforehand except in controlled laboratory experiments. Moreover, there is large uncertainty in the calculation of Q_s [26,41]. Thus, they developed a width equation by using dimensional analysis and calculated regime channel characteristics and incorporating a resistance equation, width equation, and an optimization criteria.

Singh et al. [42], influenced by the work of Deng and Zhang [43], developed a regime method by combining principles of maximum entropy and minimum energy dissipation rate (ME and MEDR).

The purpose of this work is to evaluate and compare four different extremal hypothesis-based regime methods, namely minimization of Froude number (MFN), maximum entropy and minimum energy dissipation rate (ME and MEDR), maximum flow efficiency (MFE), and Millar's method, by dividing the regime dataset into sand and gravel. All of the four methods are different in their procedure to compute regime channel characteristics which are described in Section 2. The dataset is divided into sand and gravel bed for evaluation.

2. Description of Methods

2.1. Maximum Flow Efficiency (MFE)

Huang and Nanson [28,36] defined MFE as maximum sediment transport capacity per unit available power and expressed as

$$\text{Max } F_e(\zeta) = \text{Max} \frac{Q_s}{\Omega^\alpha}(\zeta) \quad (8)$$

where F_e is a measure of flow efficiency, Ω is the total energy of flow in the form of the product of flow discharge and energy slope ($=\gamma Q_s$, where γ is the specific weight of water and Q is the bank full discharge), ζ is the width to depth ratio, and α is an exponent of less than 1.0 and also varies with bed load transport equations adopted.

Using the Manning–Strickler flow resistance Equation (9) and Meyer–Peter and Müller bed load Equation (10) modified by MFE theory, Huang et al. [27] derived regime channel width B_R given by Equation (13) and depth h_R given by Equation (14) using MFE as an optimization criteria. This method is typically representative of methods using bed load transport to calculate regime channel.

$$V = c_f \sqrt{gRS} \left(\frac{R}{D_{50}} \right)^{1/6} \text{ (Flow resistance equation)} \quad (9)$$

where V is the flow velocity (m/s), g is acceleration due to gravity (m/s^2), R is the hydraulic radius (m), S is the slope, D_{50} is median bed sediment size (m), and c_f is the frictional coefficient, which has relation with Manning’s coefficient (n), given by $c_f = \frac{D_{50}^{1/6}}{ng^{1/2}}$.

$$\varnothing = c_b(\tau_b^* - \tau_c^*)^\beta \quad (\text{Bed load equation}) \tag{10}$$

where \varnothing is the dimensionless sediment transport rate expressed by Equation (11), c_b is the coefficient whose value is 6, τ_b^* is a dimensionless flow strength parameter given by Equation (12), τ_c^* is the dimensionless critical shear stress of flow for the incipient motion of bed sediments whose value is 0.047, and β is an exponent whose value is 5/3.

$$\varnothing = \frac{q_b}{\gamma_s \sqrt{\left(\frac{\gamma_s}{\gamma} - 1\right) g D_{50}^3}} \tag{11}$$

$$\tau_b^* = \frac{\tau_o}{(\gamma_s - \gamma) D_{50}} \tag{12}$$

where q_b is the rate of bed load discharge in dry volume per unit channel width, τ_o is the shear stress of the flow and γ_s is the specific weight of the sediments.

$$B_R = \left(\frac{Q}{C_f \sqrt{gS}}\right)^{\frac{3}{8}} D_{50}^{\frac{1}{16}} \zeta_m^{\frac{3}{8}} (\zeta_m + 2)^{\frac{1}{4}} \tag{13}$$

$$h_R = \left(\frac{Q}{C_f \sqrt{gS}}\right)^{\frac{3}{8}} D_{50}^{\frac{1}{16}} \zeta_m^{-\frac{13}{8}} (\zeta_m + 2)^{\frac{1}{4}} \tag{14}$$

where ζ_m is the optimum channel width/depth ratio which can be determined by solving the Equation (15)

$$k_2 \frac{\zeta_m^{\frac{3}{8}}}{(\zeta_m + 2)^{\frac{3}{4}}} - \tau_c^* = \frac{3\beta(\zeta_m - 2)\tau_c^*}{6(1 + \beta) + (5 - 3\beta)\zeta_m} \tag{15}$$

The maximum bed load discharge can be determined by Equation (16).

$$Q_s = k_1 \zeta^{\frac{3}{8}} (\zeta + 2)^{\frac{1}{4}} \left[k_2 \frac{\zeta^{3/8}}{(\zeta + 2)^{3/4}} - \tau_c^* \right]^\beta \tag{16}$$

where k_1 and k_2 are coefficients given by Equations (17) and (18), respectively.

$$k_1 = c_b \sqrt{\left(\frac{\gamma_s}{\gamma} - 1\right) g} d^{25/16} \left(\frac{Q}{c_f \sqrt{gS}}\right)^{3/8} \tag{17}$$

$$k_2 = \frac{S^{13/16}}{\left(\frac{\gamma_s}{\gamma} - 1\right) d^{15/16}} \left(\frac{Q}{c_f \sqrt{g}}\right)^{3/8} \tag{18}$$

2.2. Minimization of Froude Number (MFN)

For calculating regime channel characteristics B_R and h_R , Yalin and Da Silva [1] used resistance Equation (19), width Equation (20), and minimization of Froude number Equation (21) as an optimization criteria. The optimization criteria of minimization of Froude number was derived

from principles of thermodynamics. In contrast to other extremal hypotheses, the bed load transport equation is supplanted by a width equation.

$$(F_r)_R = \frac{Q^2}{(gB_R^2h_R^3)} \quad (\text{Resistance equation}) \quad (19)$$

$$B_R = \alpha_B \sqrt{\frac{Q}{v_{*cr}}} \quad (\text{Width Equation}) \quad (20)$$

$$(F_r)_R = c_R^2 S_R \rightarrow \min(\text{Minimum Froude number}) \quad (21)$$

The detailed procedure for solving Equations (19)–(21) is shown in [1] (p. 95).

2.3. Maximum Entropy and Minimum Energy Dissipation Rate (ME and MEDR)

Singh et al. [44] used two hypotheses for calculating stable hydraulic geometry. The first hypothesis is that “the spatial variation of the stream power of a channel for a given discharge is accomplished by the spatial variation in channel form (flow depth and channel width) and hydraulic variables, including energy slope, flow velocity, and friction”. Using this hypothesis, they derived the following relations:

$$P_n = \frac{2n\gamma Q^3}{B^2h^{10/3}} \frac{[dn/dx]}{[d(SP)/dx]} \quad (22)$$

$$P_B = \frac{2n^2\gamma Q^3}{B^3h^{10/3}} \frac{[dB/dx]}{[d(SP)/dx]} \quad (23)$$

$$P_h = -\frac{10\gamma n^2 Q^3}{3B^2h^{13/3}} \frac{[dh/dx]}{[d(SP)/dx]} \quad (24)$$

where P_n , P_B and P_h are the proportions of the adjustment of stream power by friction, channel width, and flow depth, respectively, and n , γ , Q , SP , h , B and x are Manning’s roughness coefficient, weight density of water, flow discharge, stream power, flow depth, channel width, and the direction of flow, respectively. Then they applied the second hypothesis that is the principle of maximum entropy and minimum energy dissipation to show $P_n = P_B = P_h$, which resulted in four sets of possibilities; (1) $P_n = P_B$, (2) $P_h = P_B$, (3) $P_n = P_h$, and (4) $P_n = P_B = P_h$. These four sets of possibilities were solved to obtain a family of hydraulic geometry relations. The calibration of derived hydraulic geometry relations and morphological coefficients determination were carried out for an assumed V-shaped channel cross-section. It was found that possibility (2) $P_h = P_B$, is most prevalent in nature and it was used to validate the hypotheses. The stable hydraulic relations from possibility (2) $P_h = P_B$ are

$$B_R = 0.50z \frac{Q^{0.462}}{S^{0.231}} \quad (25)$$

$$h_R = 1.52\left(\frac{n}{z}\right)^{0.6} \frac{Q^{0.323}}{S^{0.161}} \quad (26)$$

where Q is the bankfull discharge (m^3/s), z is the stable side slope, and n is the Manning’s coefficient.

2.4. Millar’s Method

Millar and Quick [38] incorporated bank stability criteria, which are influenced by vegetation, in the model of MTC. They found that bank stability criteria have a significant influence on the hydraulic geometry of the channel with the vegetated channel being narrower, deeper, and less steep. Based on the model of Millar and Quick [38], Eaton and Millar [39] argued that extremal models which do not incorporate bank stability criteria are inappropriate for use. Millar [40] derived stable hydraulic

geometry characteristics B_R, h_R in dimensionless form using maximum sediment-transport efficiency as optimization criteria with consideration of dimensionless bankfull discharge (Q^*), slope (S), and bank strength (μ') as independent variables. The relations have the form

$$B_R^* = 28Q^{*0.7}S^{0.6}\mu'^{-1.10} \tag{27}$$

$$h_R^* = 0.125 Q^{*0.16}S^{-0.62}\mu'^{0.64} \tag{28}$$

$$\frac{B_R}{h_R} = 0.155Q^{*0.53}S^{1.23}\mu'^{-1.74} \tag{29}$$

where B_R^* is the dimensionless regime channel width ($B_R^* = B_R/D_{50}$), h_R^* is the dimensionless regime channel depth ($h_R^* = h_R/D_{50}$), Q^* is dimensionless bankfull discharge given by Equation (30), S is the slope, and μ' is the relative bank strength defined as the ratio of critical shear stress for bank to bed sediments given by Equation (31)

$$Q^* = \frac{Q}{D_{50}^2 \sqrt{gD_{50}(s-1)}} \tag{30}$$

$$\mu' = \frac{\tau_{bankc}}{\tau_{bedc}} \tag{31}$$

where s is the specific gravity of the sediment particle ($s = 2.65$), τ_{bankc} is the dimensional critical stress (Pa) for the bank sediments, and τ_{bedc} is the dimensional critical stress (Pa) for the bed sediments.

3. Data Selection

Regime channel data for sand bed, in total 266, were assembled from [27,45–47]. Each regime channel entailed observed values of bankfull discharge Q (m^3/s), median bed sediment size D_{50} (mm), width B (m), depth h (m), and slope S . Ackert [46] collected regime data from various journals and technical reports. These data were from both laboratory and field channels. Huang et al. [27] collected regime channel data from six different reaches of the middle and lower Yangtze river. Huang et al. [27] used these data to test the predictive capability of MFE. Valentine et al. [46] and Wolman and Brush Jr. [47] collected regime data from self-formed laboratory channels. The description of the sand bed data is shown in Table 1.

Table 1. Description of the Regime Data.

Observed Variables	Range	Type of Bed	References
Bankfull Discharge $Q, m^3/s$	0.004–46,000	Sand	[27,45–47]
Median Bed Sediment Size D_{50}, mm	0.07–2		
Width B, m	0.35–2190		
Depth h, m	0.02–23		
Slope $S, \%$	0.78–0.00152		
Bankfull Discharge $Q, m^3/s$	0.697–424	Gravel	[2,17,48,49]
Median Bed Sediment Size D_{50}, mm	13.9–175.8		
Width B, m	2.32–83.8		
Depth h, m	0.201–3.21		
Slope $S, \%$	0.088–2.6		
Vegetation Type	I, II, III, IV, Thin, Thick		

Regime channel data for gravel bed, in total 127, were collected from [2,17,48,49]. Each regime channel data entailed observed values of bankfull discharge Q (m^3/s), median bed sediment size D_{50} (mm), width B (m), depth h (m), and slope S . In addition to these observations, information about bank vegetation was also present. Hey et al. [2] and Davidson and Hey [17] divided the bank vegetation into four different classes, namely Type I, which represented grassy banks with no trees or bushes; Type II, 1–5% tree/shrub cover; Type III, 5–50% tree/shrub cover; and Type IV, greater than 50%

tree/shrub cover. Similarly, Andrews [48] divided the bank vegetation into thin and thick categories. The description of the gravel data is shown in Table 1.

In addition to the observed values, some more parameters like Manning’s n and critical side slope z are needed in the methods ‘ME and MEDR.’ These were calculated based on observed values. For example, Manning’s n was calculated using observed bankfull discharge, width, depth, and slope [39] while critical side slope z was determined as in [43].

4. Results and Discussion

4.1. For Sand Bed

Predicted regime channel widths B_R are plotted against observed widths B_R , with \log_{10} -transformation applied to both, in Figure 1, and predicted regime channel depths h_R are plotted against observed depths h_R in Figure 2. Similarly, the disparity ratio, defined as the ratio of predicted to observed value, for width B_R and depth h_R , is plotted against bankfull discharge in Figures 3 and 4, respectively. The data used are from sand bed channels obtained from [27,45–47]. Of the four methods, Miller’s method could not be used because it uses a bed load equation developed only for gravel beds.

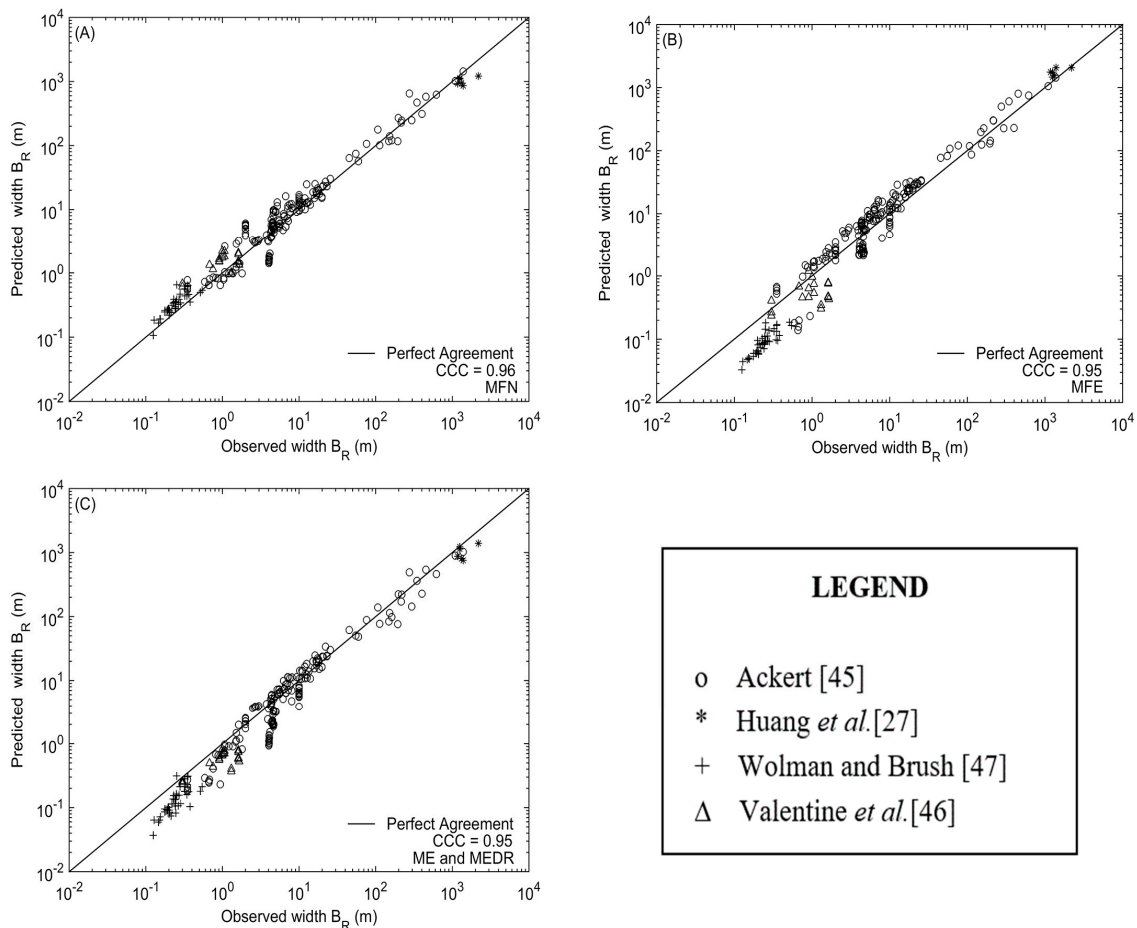


Figure 1. Comparison of predicted and observed widths B_R for sand bed channels [27,45–47]. (A) MFN; (B) MFE; (C) ME and MEDR.

Concordance correlation coefficient (CCC) [50] is used to measure the agreement between predicted and observed values. The value of CCC lies between 0 and 1. Mathematically, CCC is given by

$$CCC = \frac{2\sigma_1\sigma_2\sigma_{12}}{\sigma_1^2 + \sigma_2^2 + (\mu_1 - \mu_2)^2} \quad (32)$$

where σ_1 is the standard deviation of the observed values, σ_2 is the standard deviation of the predicted values, μ_1 is the mean of the observed values, μ_2 is the mean of the predicted values, and σ_{12} is the Pearson correlation coefficient between the observed and predicted values. In addition to CCC, the percentages of predicted widths and depths falling under a specific error range (say $\pm 30\%$) is calculated to assess the accuracy of the methods. This is important because sediment-transport-related data inevitably plot with a certain degree of scattering along a perfect agreement line. The statistics computed for the three methods are shown in Table 2.

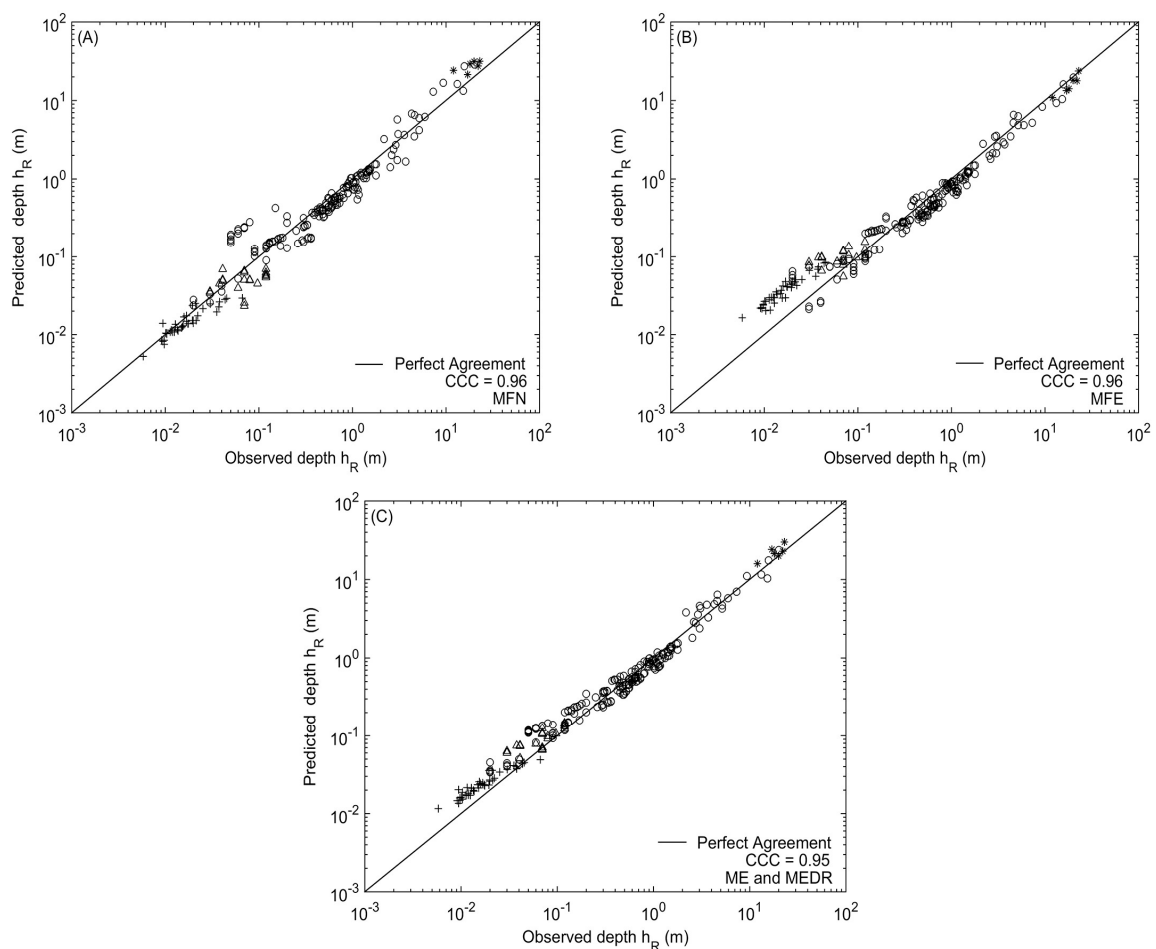


Figure 2. Comparison of predicted and observed depth h_R for sand bed channels [27,45–47]. (A) MFN; (B) MFE; (C) ME and MEDR. Same legend as on Figure 1 applies here.

Table 2. Statistics computed for MFE, MFN, and ‘ME and MEDR’ based on sand bed data.

Method	CCC		Width B_R		Depth h_R		Predicted
	Width B_R	Depth h_R	30% Error Range	50% Error Range	30% Error Range	50% Error Range	$\frac{B_R}{h_R}$
MFN	0.96	0.96	59%	75%	72%	87%	6.8–63
MFE	0.95	0.96	26%	56%	51%	72%	2–154
ME and MEDR	0.95	0.95	44%	70%	61%	77%	4.2–61

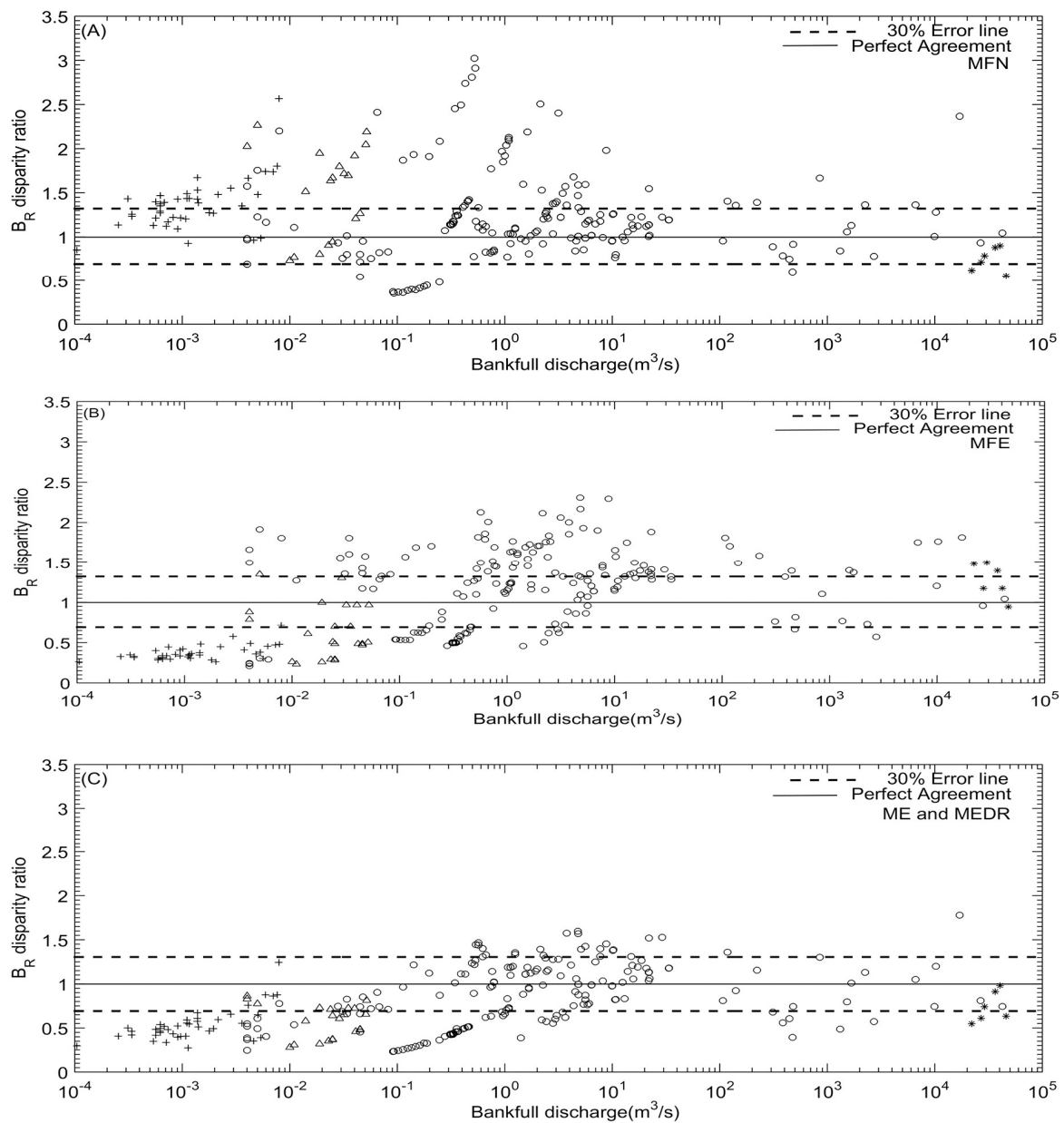


Figure 3. Scatter plot of disparity ratio B_R against bankfull discharge for sand bed channels [27,45–47]. (A) MFN; (B) MFE; (C) ME and MEDR. Same legend as on Figure 1 applies here.

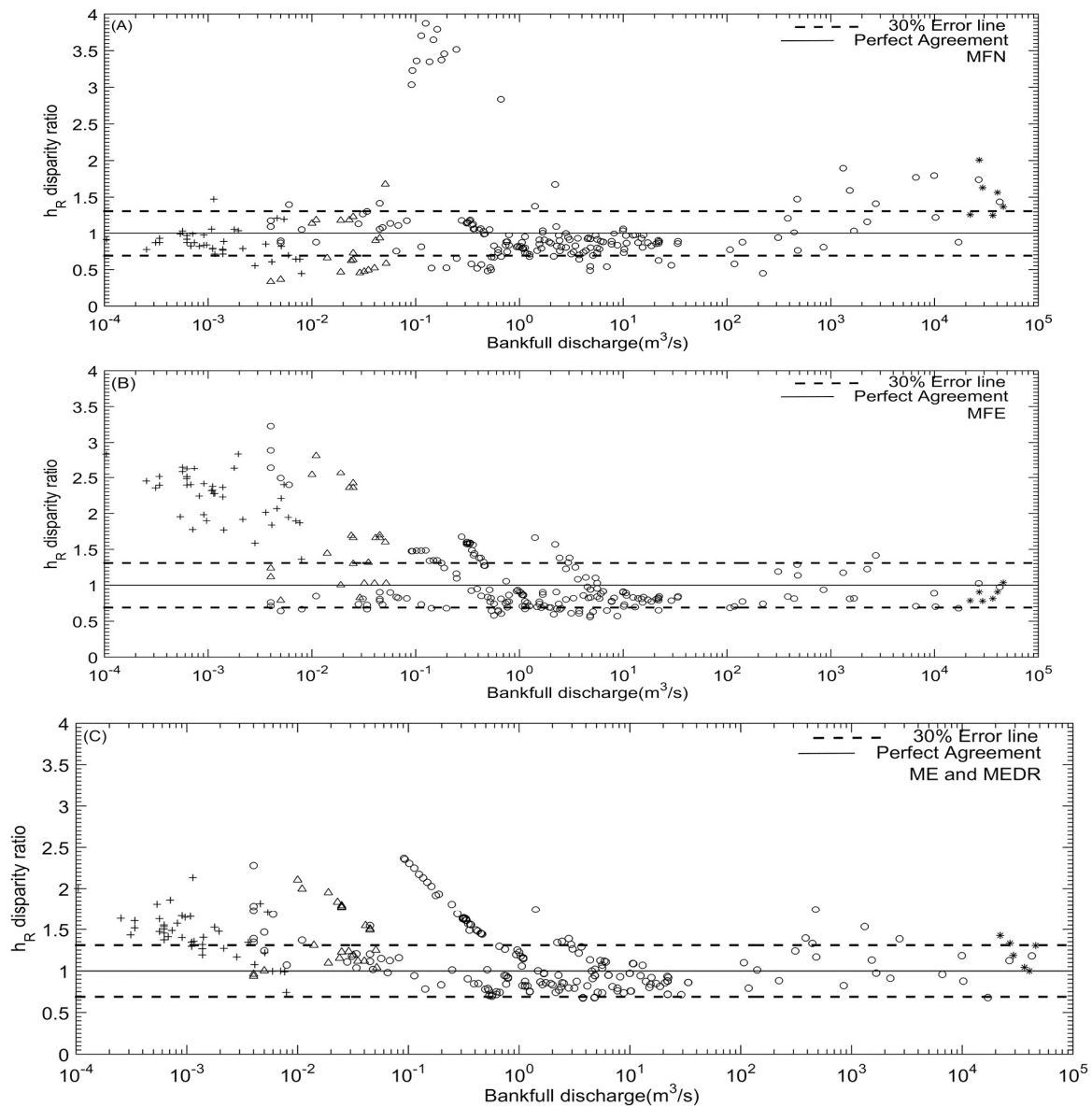


Figure 4. Scatter plot of disparity ratio h_R against bankfull discharge for sand bed channels [27,45–47]. (A) MFN; (B) MFE; (C) ME and MEDR. Same legend as on Figure 1 applies here.

4.1.1. Regime Channel Width

The predicted widths by MFN are well scattered around the perfect agreement line $y = x$ (Figure 1A) with CCC value of 0.96. MFE (Figure 1B) and ‘ME and MEDR’ (Figure 1C) underpredict the regime channel width when the observed width is less than 1m. The CCC value for MFE is 0.95, and that for ‘ME and MEDR’ is 0.95. Also, the percentage of predicted width for MFN falling within $\pm 30\%$ error range is 59% while that for MFE is 26% and ‘ME and MEDR’ is 44% (see Table 2). Similarly, the predicted width to depth ratio for MFN is in the range of 6.8–63 while that for MFE is 2–154, and ‘ME and MEDR’ is 4.2–61 (see Table 2). It is clear from observation of the figures and statistics that MFN gives high accuracy for prediction of regime channel width.

4.1.2. Regime Channel Depth

The predicted depths by MFN are well scattered around the perfect agreement line $y = x$ (Figure 2A) with CCC value of 0.96. Also, the percentage of predicted depths for MFN falling

within $\pm 30\%$ error range is 75%. MFE (Figure 2B) and ‘ME and MEDR’ (Figure 2C) overpredict the regime channel depth when the observed width is less than 0.1 m. The CCC value for MFE is 0.95, and that for ‘ME and MEDR’ is 0.95. Also, the percentage of predicted depth within $\pm 30\%$ error range for MFE is 56% while that for ‘ME and MEDR’ is 70% (see Table 2). It is clear from observation of the figures and statistics that MFN gives high accuracy for prediction of regime channel depth.

4.1.3. Underprediction of Width and Overprediction of Depth by MFE

MFE underpredicts the width and overpredicts the depth for certain data points portrayed by +, Δ (Figures 1B and 2B). These data points are from [46,47]. Such results occurred because of these data points’ width/depth ratio $\zeta_m \rightarrow 2$ in Equation (15), which also gives bed load $Q_s \rightarrow 0$ in Equation (16). The width/depth ratio $\zeta_m \rightarrow 2$ because for these data points, the shear stress on the bed at regime state is either equal to or less than the critical shear stress for the incipient motion. This is the result of the linear relationship between shear stress and the width/depth ratio [51] given by

$$\frac{\tau_o - \tau_c}{\tau_c} = \chi[\zeta_m - (\zeta_m)_c] \tag{33}$$

where χ is a coefficient, $(\zeta_m)_c$ is the width/depth ratio at the critical state of motion whose value is 2. However, Eaton and Millar [39] and Millar [40] have argued that this low prediction of width/depth ratio is due to lack of bank strength or bank stability criteria in the formulation of MFE.

4.2. For Gravel Bed

Predicted regime channel widths B_R are compared with observed width with \log_{10} -transformation applied to both in Figure 5 and predicted regime channel depths h_R are compared with observed depth in Figure 6. Similarly, the disparity ratio for width B_R and depth h_R is plotted against bankfull discharge in Figures 7 and 8, respectively. All of the four methods are applicable here. Regime data compiled by Hey et al. [2], Andrews [48], Davidson and Hey [17], and Mueller et al. [49] are used. The vegetation classes as described in Section 3 are again divided into two categories, namely sparse vegetation which contains Type I, II, and Thin, and dense vegetation which contains Type III, IV, and Thick, as in [40]. It is essential to divide the regime data into sparse and dense vegetation classes because bank strength μ' , which depends upon vegetation density in Millar’s method, is difficult to measure. However, for sparse vegetation class, $\mu' = 1$ can be considered [40]. Here only the sparse vegetation category which consists of 82 sets of regime data is used.

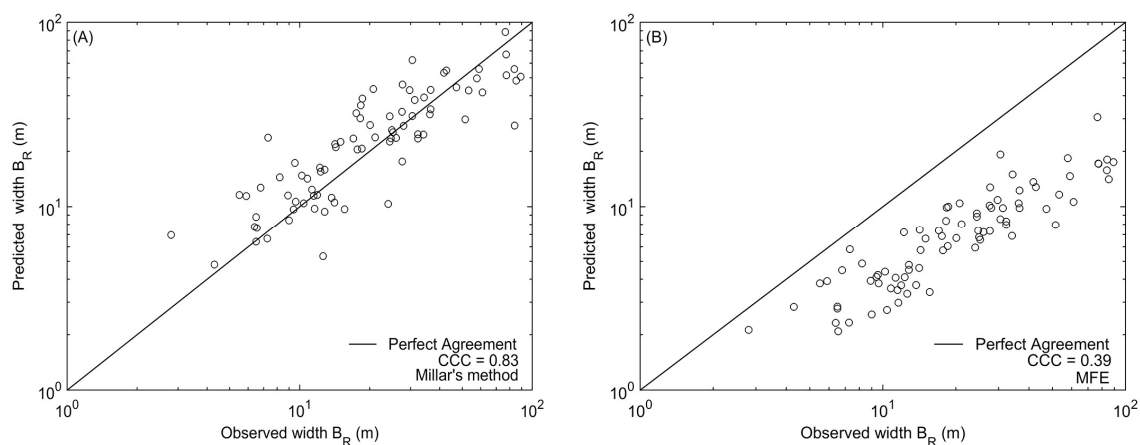


Figure 5. Cont.

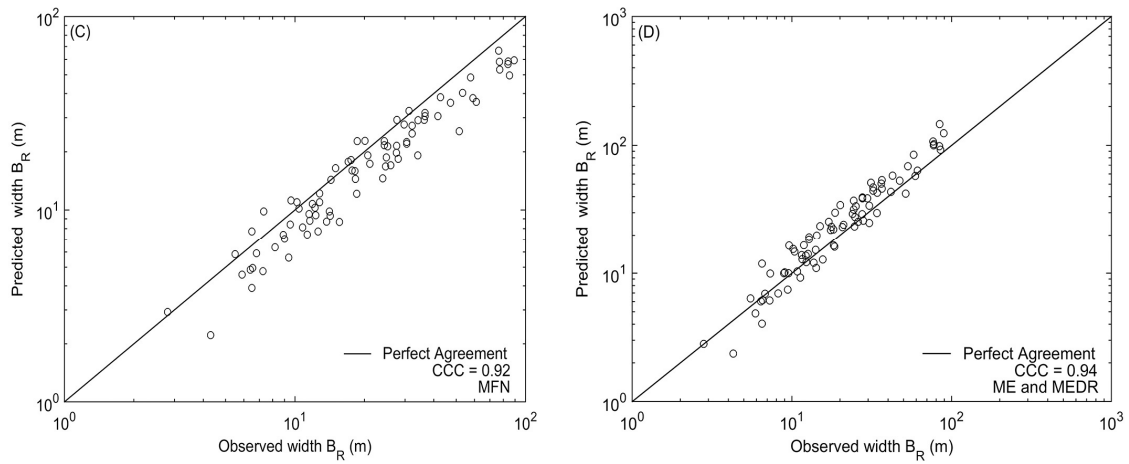


Figure 5. Comparison of predicted and observed width B_R for gravel bed channels [2,17,48,49], (A) Millar’s Method; (B) MFE; (C) MFN; (D) ME and MEDR.

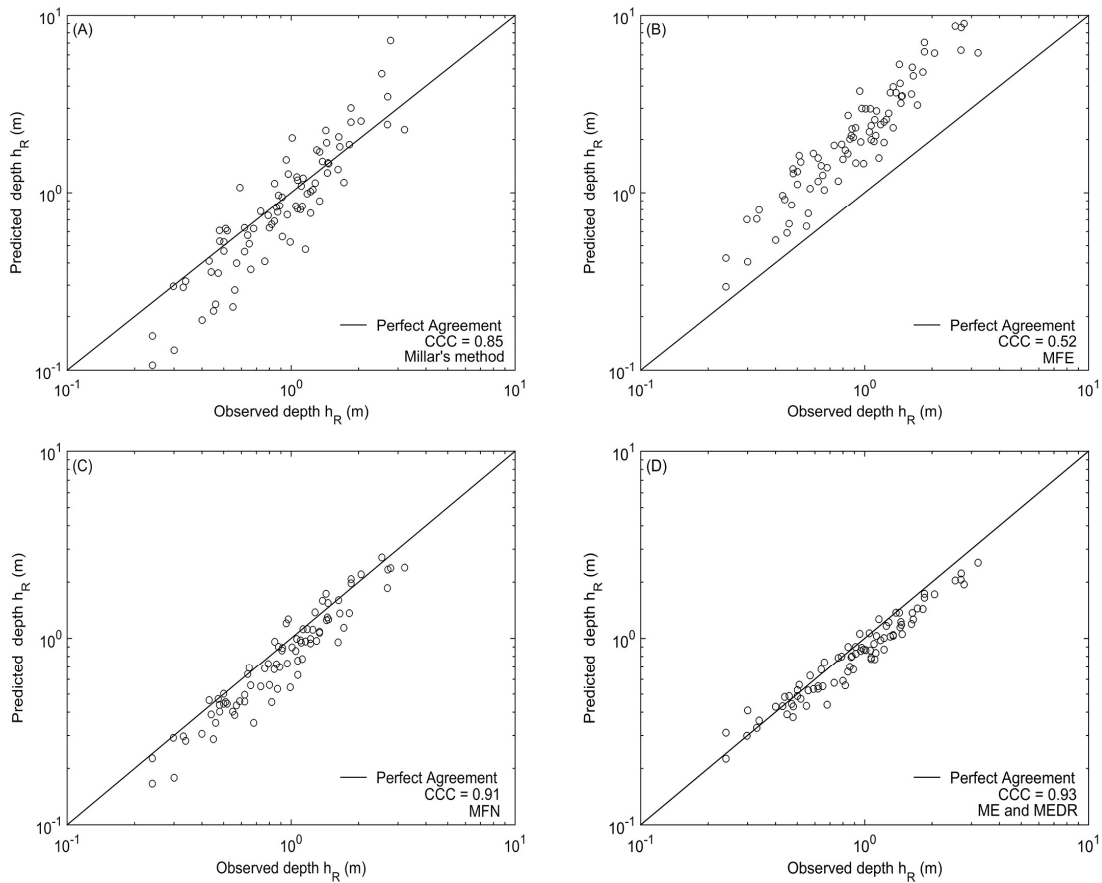


Figure 6. Comparison of predicted and observed depth h_R for gravel bed channels [2,17,48,49]. (A) Millar’s Method; (B) MFE; (C) MFN; (D) ME and MEDR.

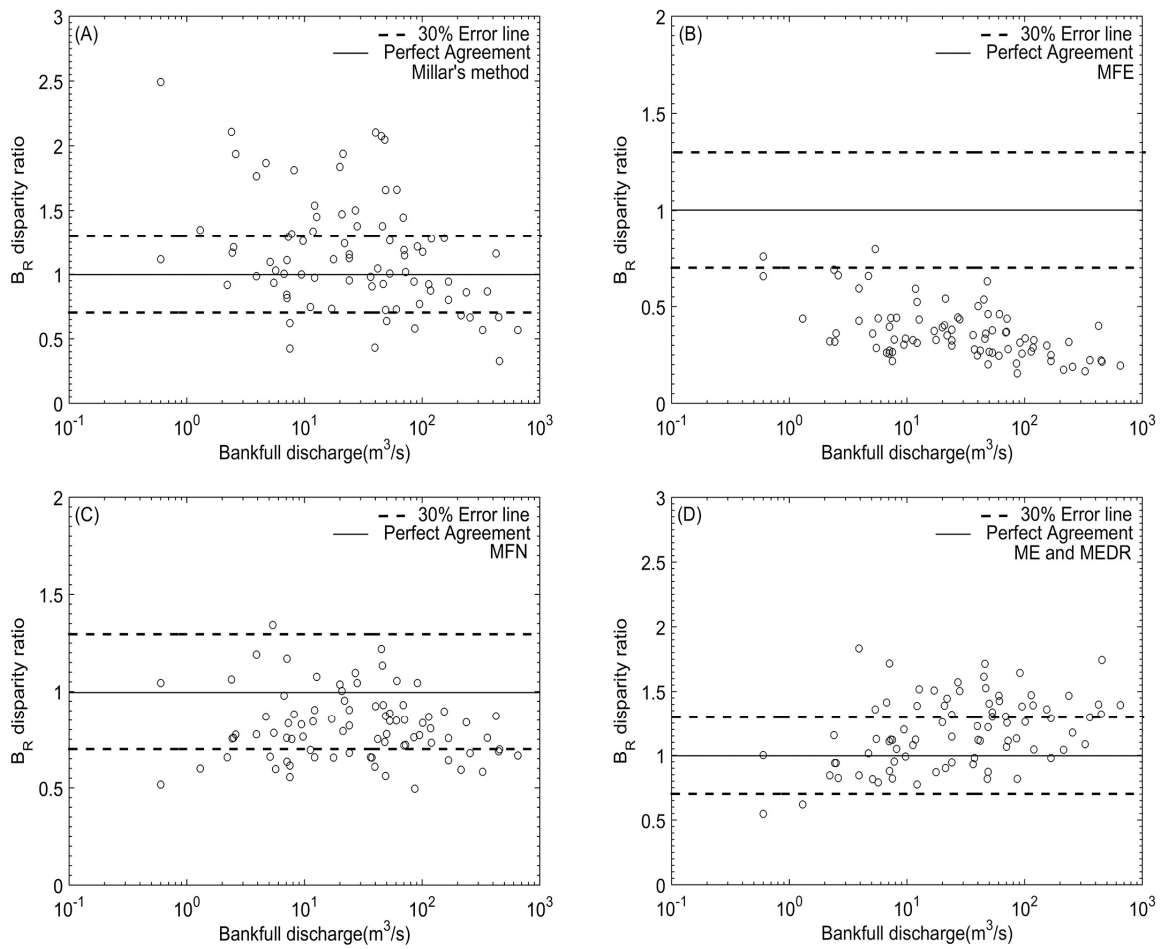


Figure 7. Scatter plot of disparity ratio B_R against bankfull discharge for gravel bed channels [2,17,48,49]. (A) Millar's Method; (B) MFE; (C) MFN; (D) ME and MEDR.

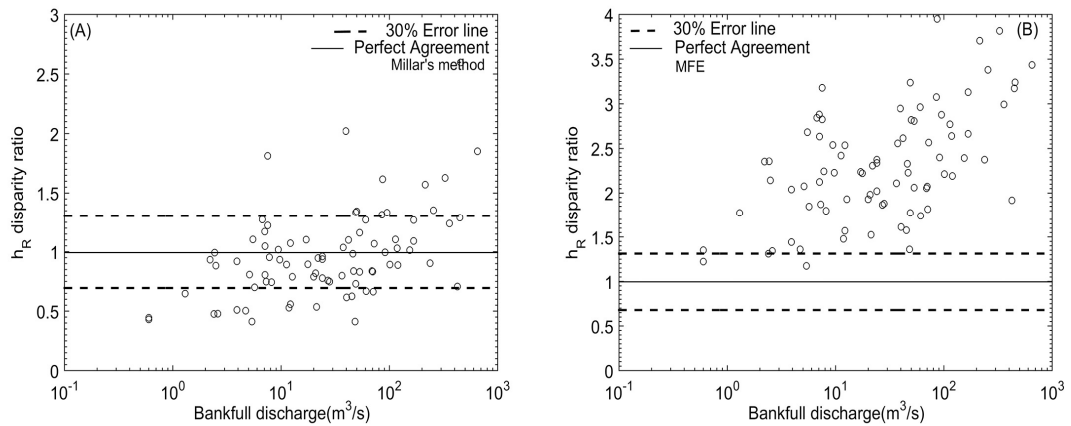


Figure 8. Cont.

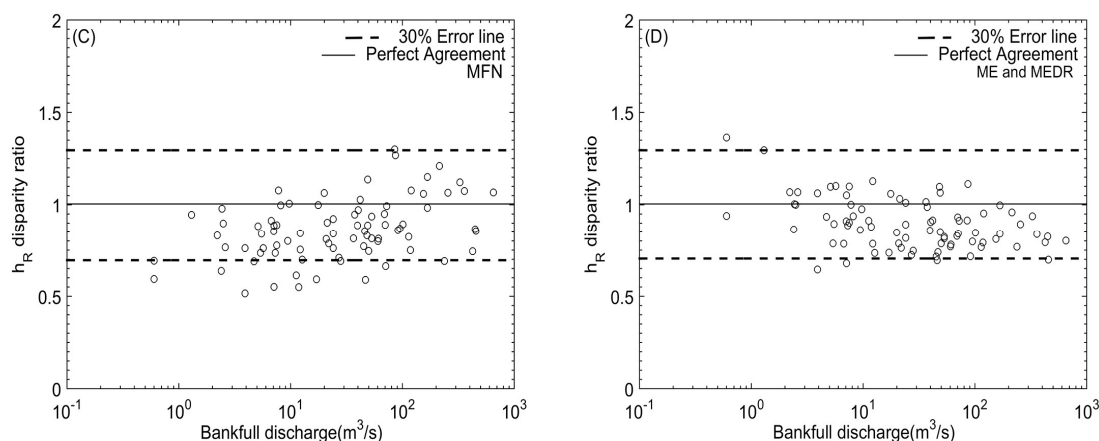


Figure 8. Scatter plot of disparity ratio h_R against bankfull discharge for gravel bed channels [2,17,48,49]. (A) Millar’s Method; (B) MFE; (C) MFN; (D) ME and MEDR.

Regime Channel Width and Depth

MFE gives the poorest prediction for regime channel width and depth with CCC values for width 0.39 and depth 0.52. Similarly, the percentage of predicted width and depth within $\pm 30\%$ error range is 3% and 3%, respectively. Also, the predicted width to depth ratio is very narrow and is in the range of 2–12. Millar’s method gives a moderately good prediction for regime channel width and depth with CCC values for width 0.83 and depth 0.85. The percentage of predicted width and depth within $\pm 30\%$ error range is 57% and 66%, respectively. The predicted width to depth ratio by Millar’s method is in the range of 4–130. MFN and ‘ME and MEDR’ give an excellent prediction for regime channel width and depth. For MFN the CCC value for width is 0.92 and for depth is 0.91, while for ‘ME and MEDR’ the CCC value for width is 0.94 and for depth is 0.93. Similarly, the percentage of predicted width and depth within $\pm 30\%$ error range is 70% and 82%, respectively, for MFN while for ‘ME and MEDR’ it is 60% and 93%, respectively.

MFE underpredicts the width and overpredicts the depth (Figures 5B and 6B). The predicted width/depth ratio is in the range of 2–12 (see Table 3) which is very low for gravel bed channels because natural gravel tends to have a width/depth ratio greater than 10 [40]. This low prediction of width/depth ratio may be due to a linear relationship between shear stress and width/depth ratio as governed by Equation (33). When the shear stress on the bed surface decreases, then accordingly the width/depth ratio decreases. Nevertheless, Eaton and Millar [39] and Millar [40] have asserted that this low prediction of width/depth ratio is because MFE does not account for bank stability or bank strength criteria in its formulation. Moreover, they argue that optimization or extremal models which are not comprised of bank stability are inappropriate for use in the prediction for regime channels.

Table 3. Statistics computed for Millar’s method, MFE, MFN, and ‘ME and MEDR’ based on sparse gravel data.

Method	CCC		Width B_R		Depth h_R		Predicted
	Width B_R	Depth h_R	30% Error Range	50% Error Range	30% Error Range	50% Error Range	$\frac{B_R}{h_R}$
Millar’s method	0.83	0.85	57%	76%	66%	84%	4–130
MFE	0.39	0.52	3%	16%	3%	11%	2–12
MFN	0.92	0.91	70%	98%	82%	100%	12.5–28.9
ME and MEDR	0.94	0.93	60%	86%	93%	100%	11.4–75

However, methods of MFN and ‘ME and MEDR’ do not show such bias towards low prediction of width/depth ratio (see Table 3.) and also do not account for bank strength. The predicted width/depth

ratio is in the range of 12.5–28.9 for MFN and 11.4–75 for ‘ME and MEDR’. This may be because MFN and ‘ME and MEDR’ both lack the bed load transport equation as a contrast to MFE for computation of regime channel. MFN uses a width equation instead of the sediment transport equation, while ‘ME and MEDR’ use bankfull discharge, slope, Manning’s coefficient (n), and side slope (z) to calculate regime channel dimensions. The results obtained by MFE and ‘ME and MEDR’ can also be corroborated by empirical regime relations for gravel bed rivers established by Davidson and Hey [17]. They found that regime channel width and depth are independent of bed load but influenced by vegetation. Thus the claim of Eaton and Millar [39] that regime models not comprised of bank strength are inappropriate for use is found to be false because both MFN and ‘ME and MEDR’ give a very high accuracy of prediction for regime channel width and depth.

4.3. Influence of Vegetation in Hydraulic Geometry

Bank vegetation has significant influence on the hydraulic geometry relations of the alluvial channels [2,39,40,48,52]. Bank vegetation affects the coefficient of the hydraulic geometry relations, not the exponent. Strong bank vegetation results in narrow, deep, and steep alluvial channels [10].

In order to show the influence of the vegetation on the regime models of MFN and ‘ME and MEDR’, a similar framework as in [40] is used here. The disparity ratio for width B_R and depth h_R is plotted against bankfull discharge in Figures 9 and 10, respectively. Millar [40] used bank strength $\mu' = 1$ in Equations (27) and (28) to calculate regime channel widths and depths and subsequently found that predicted regime channel widths for the denser vegetation class were wider than their observed counterparts. The predicted depths were shallower than their observed counterparts. These results are vivid in Figure 9A in which the B_R disparity ratio for width is greater than 1 for denser vegetation and in Figure 10A, the h_R disparity ratio for width is less than 1 for denser vegetation. MFN (Figures 9B and 10B) and ‘ME and MEDR’ (Figures 9C and 10C) also give similar results. This signifies that regime models of MFN and ‘ME and MEDR’ should also incorporate bank vegetation in their computation.

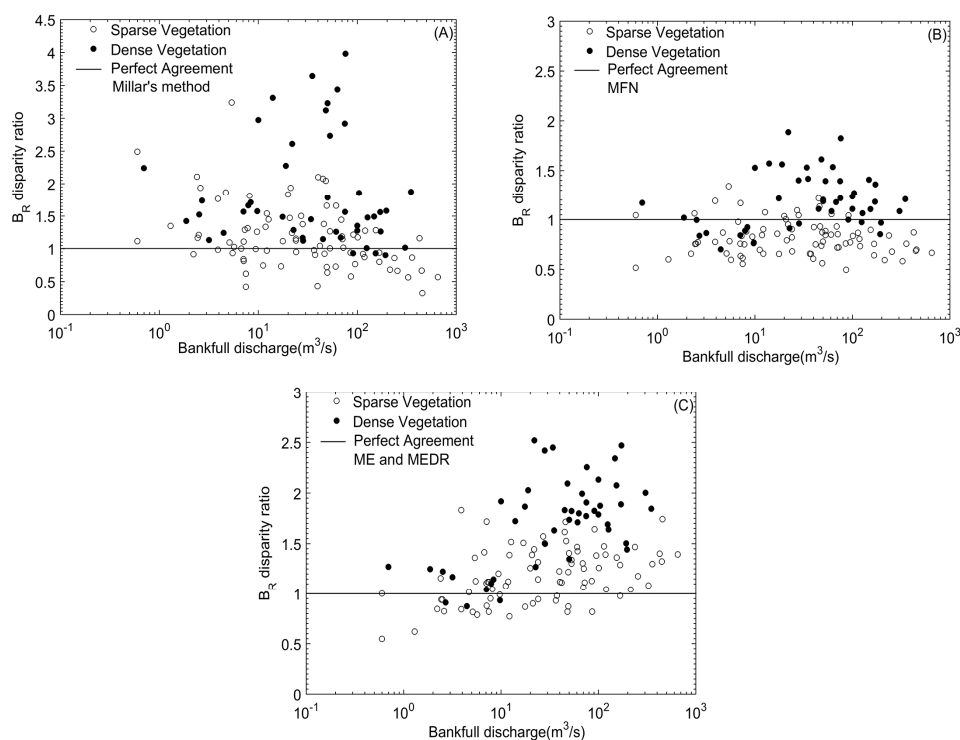


Figure 9. Scatter plot of disparity ratio B_R against bankfull discharge for gravel bed channels [2,17,48,49]. (A) Millar’s Method; (B) MFN; (C) ME and MEDR.

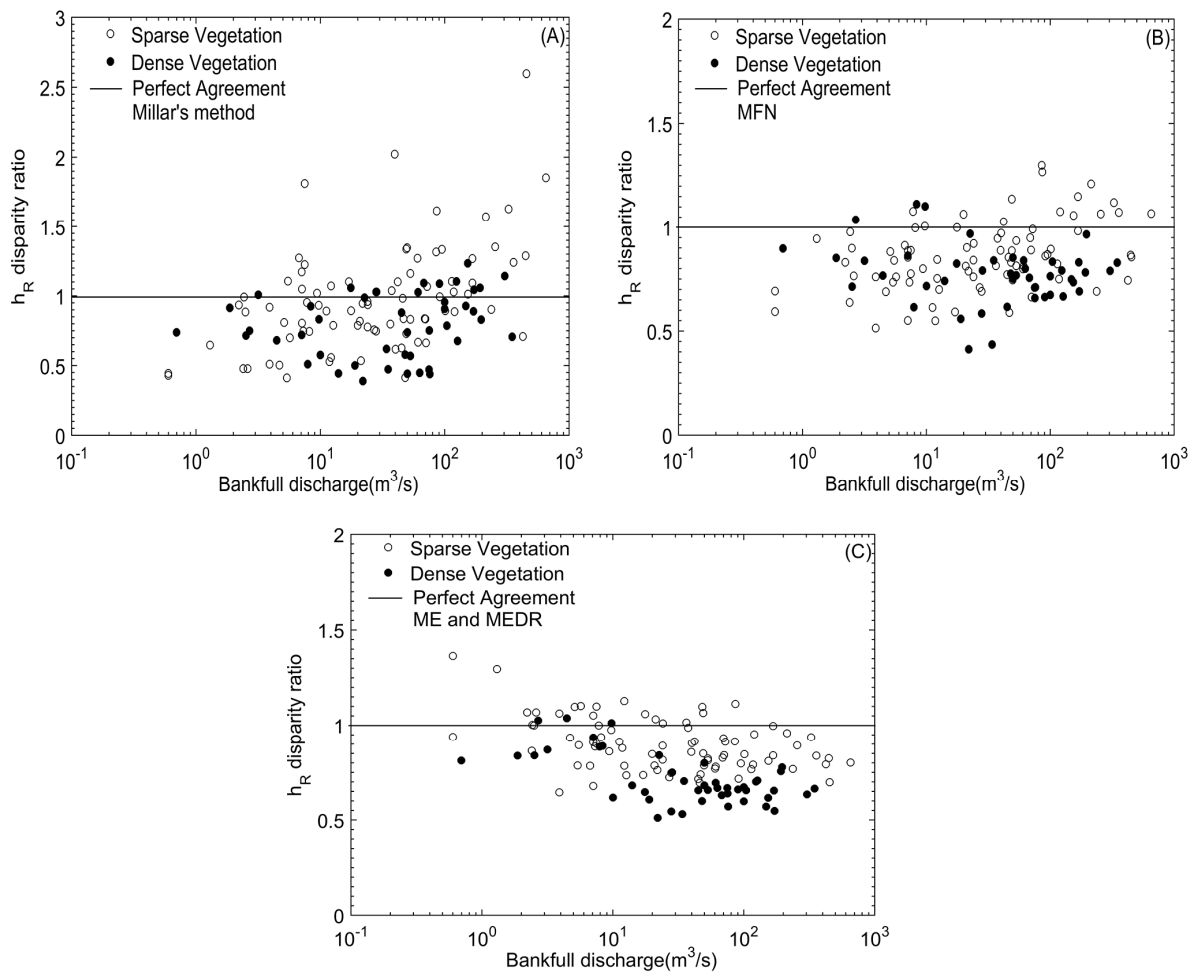


Figure 10. Scatter plot of disparity ratio h_R against bankfull discharge for gravel bed channels [2,17,48,49]. (A) Millar's Method; (B) MFN; (C) ME and MEDR.

5. Conclusions

Four extremal hypothesis-based regime methods, namely, minimization of Froude number (MFN), maximum flow efficiency (MFE), maximum entropy and minimum energy dissipation rate (ME and MEDR), and Millar's method, are evaluated and compared by dividing regime channel data into sand and gravel beds. The regime channel data are obtained from various published journal articles.

For sand bed channels, MFN gives a very high accuracy of prediction for regime channel width and depth. This method can be used for river restoration works or to determine channel changes in rivers due to natural or anthropogenic activities. Also, MFN provides a unique advantage among other extremal methods in that bed load is not required to compute regime channel width and depth for both sand and gravel beds. It is important to know that bed load is challenging to measure [40]. MFN requires only bankfull discharge and bed sediment size to compute regime channel characteristics.

The claim that regime models which do not explicitly account for bank strength or bank stability are inappropriate for use is shown false since both MFN and 'ME and MEDR' give a very high accuracy of prediction for regime channel width and depth for gravel bed channels. Therefore, these two methods can be used for regime channel computation when the bank is unvegetated and consists of loose gravel (i.e., Bank strength $\mu' = 1$). However, when the bank has a significant amount of vegetation, these two methods will give erroneous results.

Predicted regime channel widths and depths obtained by MFN and ‘ME and MEDR’ are influenced by bank vegetation. However, these two methods do not account for vegetation influence in their computation. Additional study is required to account for vegetation influence in both MFN and ‘ME and MEDR’. For example, width equation can be redefined in MFN to account for vegetation.

More regime data for both sand and gravel bed is required to evaluate regime methods so attempts should be made to collect data from a large number of sources. This is because regime channel data from the individual source are not fully reliable [1] (p. 93).

Acknowledgments: This research is supported by the National Key R&D Program of China (2016YFC0402501), the NSFC (51479071), the 111 project (B17015, B12032) and the Priority Academic Program Development of Jiangsu Higher Education Institutions (PAPD).

Author Contributions: All of the authors have contributed to this paper. Ishwar Joshi analyzed the data and wrote the manuscript, Wenhong Dai is the corresponding author and he formulated the idea, and Ahmed Bilal, Akhanda Raj Upreti, and Ziming He performed the technical review.

Conflicts of Interest: The authors declare no conflict of interest.

References

1. Yalin, M.S.; Da Silva, A.M.F. *Fluvial Processes*; IAHR: Delft, The Netherlands, 2001.
2. Hey, R.D.; Thorne, C.R. Stable Channels With Mobile Gravel Beds. *J. Hydraul. Eng.* **1986**, *112*, 671–689. [[CrossRef](#)]
3. Cao, S.; Knight, D.W. Design for hydraulic geometry of alluvial channels. *J. Hydraul. Eng.* **1998**, *124*, 484–492. [[CrossRef](#)]
4. Eaton, B.C.; Millar, R.G. Predicting gravel bed river response to environmental change: The strengths and limitations of a regime-based approach. *Earth Surf. Process. Landf.* **2016**. [[CrossRef](#)]
5. Eaton, B.C.; Moore, R.D.; Giles, T.R. Forest fire, bank strength and channel instability: The “unusual” response of Fishtrap Creek, British Columbia. *Earth Surf. Process. Landf.* **2010**, *35*, 1167–1183. [[CrossRef](#)]
6. Simon, A.; Thorne, C.R. Channel adjustment of an unstable coarse-grained stream: opposing trends of boundary and critical shear stress, and the applicability of extremal hypotheses. *Earth Surf. Process. Landf.* **1996**, *21*, 155–180. [[CrossRef](#)]
7. Julien, P.Y. Downstream hydraulic geometry of alluvial rivers. *IAHS-AISH Proc. Rep.* **2014**, *367*, 3–11. [[CrossRef](#)]
8. ASCE Task Committee. River Width Adjustment. I: Processes and Mechanisms. *J. Hydraul. Eng.* **1998**, *124*, 881–902.
9. Gleason, C.J. Hydraulic geometry of natural rivers: A review and future directions. *Prog. Phys. Geogr.* **2015**, *39*, 337–360. [[CrossRef](#)]
10. Eaton, B.C. Hydraulic Geometry: Empirical Investigations and Theoretical Approaches. *Treatise Geomorphol.* **2013**, *9*, 313–329. [[CrossRef](#)]
11. Paik, K.; Kumar, P. Optimality approaches to describe characteristic fluvial patterns on landscapes. *Philos. Trans. R. Soc. Lond. B Biol. Sci.* **2010**, *365*, 1387–1395. [[CrossRef](#)] [[PubMed](#)]
12. Singh, V.P. On the theories of hydraulic geometry. *Int. J. Sediment Res.* **2004**, *18*, 196–218.
13. Nanson, G.C.; Huang, H.Q. Least action principle, equilibrium states, iterative adjustment and the stability of alluvial channels. *Earth Surf. Process. Landf.* **2008**, *33*, 923–942. [[CrossRef](#)]
14. Kennedy, R.G. The prevention of silting in irrigation canals. (including appendix). In *Minutes of the Proceedings of the Institution of Civil Engineers*; Thomas Telford-ICE Virtual Library: Scotland, UK, 1895; Volume 119, pp. 281–290.
15. Lacey, G. Stable channels in alluvium (includes appendices). In *Minutes of the Proceedings of the Institution of Civil Engineers*; Thomas Telford-ICE Virtual Library: Scotland, UK, 1930; Volume 229, pp. 259–292.
16. Blench, T. *Mobile-Bed Fluviology; a Regime Theory Treatment of Canals and Rivers for Engineers and Hydrologists*; University of Alberta Press: Edmonton, AB, Canada, 1969.
17. Davidson, S.K.; Hey, R.D. Regime Equations for Natural Meandering. *J. Hydraul. Eng.* **2011**, *137*, 894–910. [[CrossRef](#)]

18. Lane, E.W. Progress report on studies on the design of stable channels by the Bureau of Reclamation. In Proceedings of the American Society of Civil Engineers, New York, NY, USA, 20 October 1953; Volume 79, pp. 1–31.
19. Parker, G. Self-formed straight rivers with equilibrium banks and mobile bed. Part 1. The sand-silt river. *J. Fluid Mech.* **1978**, *89*, 109–125. [[CrossRef](#)]
20. Parker, G. Self-formed straight rivers with equilibrium banks and mobile bed. Part 2. Part 2. The gravel river. *J. Fluid Mech.* **1978**, *89*, 127–146. [[CrossRef](#)]
21. Ikeda, S.; Parker, G.; Kimura, Y. Stable width and depth of straight gravel rivers with heterogeneous bed materials. *Water Resour. Res.* **1988**, *24*, 713–722. [[CrossRef](#)]
22. Ikeda, S.; Izumi, N. Width and depth of self-formed straight gravel rivers with bank vegetation. *Water Resour. Res.* **1990**, *26*, 2353–2364. [[CrossRef](#)]
23. Farias, H.D.; Pilan, M.T.; Mattar, M.T.; Pece, F.J. Regime width of alluvial channels: Conciliation of several approaches. In Proceedings of the ICHE Conference, Cottbus, Germany, 1998.
24. Khodashenas, S.R. Threshold gravel channels bank profile: A comparison among 13 models. *Int. J. River Basin Manag.* **2016**, *5124*, 337–344. [[CrossRef](#)]
25. Griffiths, G.A. Extremal Hypotheses for River Regime: An Illusion of Progress. *Water Resour. Res.* **1984**, *20*, 113–118. [[CrossRef](#)]
26. Chang, H.H. *Fluvial Processes in River Engineering*; Wiley Interscience: New York, NY, USA, 1988; ISBN 0894647377.
27. Huang, H.Q.; Deng, C.; Nanson, G.C.; Fan, B.; Liu, X.; Liu, T.; Ma, Y. A test of equilibrium theory and a demonstration of its practical application for predicting the morphodynamics of the Yangtze River. *Earth Surf. Process. Landforms* **2014**, *39*, 669–675. [[CrossRef](#)]
28. Huang, H.E.Q.; Nanson, G.C. Hydraulic geometry and maximum flow efficiency as products of the principle of least action. *Earth Surf. Process. Landforms* **2000**, *16*, 1–16. [[CrossRef](#)]
29. Pickup, G. Adjustment of stream-channel shape to hydrologic regime. *J. Hydrol.* **1976**, *30*, 365–373. [[CrossRef](#)]
30. Kirkby, M.J. *Maximum Sediment Efficiency as a Criterion for Alluvial Channels*; University of Leeds, School of Geography: Leeds, UK, 1976.
31. White, W.R.; Bettess, R.; Paris, E. Analytical approach to river regime. *J. Hydraul. Div.* **1982**, *108*, 1179–1193.
32. Chang, H. Design of stable alluvial canals in a system. *J. Irrig. Drain. Eng.* **1985**, *1*, 36–43. [[CrossRef](#)]
33. Yang, C.T.; Song, C.C.S.; Woldenberg, M.J. Hydraulic geometry and minimum rate of energy dissipation. *Water Resour. Res.* **1981**, *17*, 1014–1018. [[CrossRef](#)]
34. Yang, C.T. Minimum unit stream power and fluvial hydraulics. *J. Hydraul. Div.* **1976**, *102*, 919–934.
35. Davies, T.R.H.; Sutherland, A.J. Extremal hypotheses for river behavior. *Water Resour. Res.* **1983**, *19*, 141–148. [[CrossRef](#)]
36. Huang, H.Q.; Nanson, G.C. A stability criterion inherent in laws governing alluvial channel flow. *Earth Surf. Process. Landforms* **2002**, *27*, 929–944. [[CrossRef](#)]
37. Huang, H.Q.; Chang, H.H.; Nanson, G.C. Minimum Energy as the General Form of Critical Flow and Maximum Flow Efficiency and for explaining Variations in River Channel Pattern. *Water Resour. Res.* **2004**, *40*, W04502. [[CrossRef](#)]
38. Millar, R.G.; Quick, M.C. Effect of Bank Stability on Geometry of Gravel Rivers. *J. Hydraul. Eng.* **1993**, *119*, 1343–1363. [[CrossRef](#)]
39. Eaton, B.C.; Millar, R.G. Optimal alluvial channel width under a bank stability constraint. *Geomorphology* **2004**, *62*, 35–45. [[CrossRef](#)]
40. Millar, R.G. Theoretical regime equations for mobile gravel-bed rivers with stable banks. *Geomorphology* **2005**, *64*, 207–220. [[CrossRef](#)]
41. Barry, J.J. *Bed Load Transport in Gravel-Bed Rivers*; University of Idaho: Moscow, ID, USA, 2007.
42. Singh, V.P.; Yang, C.T.; Deng, Z.-Q. Downstream hydraulic geometry relations: 2. Calibration and testing. *Water Resour. Res.* **2003**, *39*. [[CrossRef](#)]
43. Deng, Z.; Zhang, K. Morphologic equations based on the principle of maximum entropy. *Int. J. Sediment Res.* **1994**, *9*, 31–46.
44. Singh, V.P.; Yang, T.C.; Deng, Z.Q. Downstream hydraulic geometry relations: 1. Theoretical development. *Water Resour. Res.* **2003**, *39*. [[CrossRef](#)]

45. Ackert, S.F. A Study of Different Methods for Determination of Regime Channel Geometry with Application to Streams in Southwestern Ontario. Master's Thesis, University of Windsor, Windsor, ON, Canada, 2000.
46. Valentine, E.M.; Benson, I.A.; Nalluri, C.; Bathurst, J.C. Regime theory and the stability of straight channels with bankfull and overbank flow. *J. Hydraul. Res.* **2001**, *39*, 259–268. [[CrossRef](#)]
47. Wolman, M.G.; Brush, L.M., Jr. *Factors Controlling the Size and Shape of Stream Channels in Coarse Noncohesive Sands*; US Government Printing Office: Washington, DC, USA, 1961.
48. Andrews, E.D. Bed-material entrainment and hydraulic geometry of gravel-bed rivers in Colorado. *Geol. Soc. Am. Bull.* **1984**, *95*, 371–378. [[CrossRef](#)]
49. Mueller, E.R.; Pitlick, J.; Nelson, J.M. Variation in the reference Shields stress for bed load transport in gravel-bed streams and rivers. *Water Resour. Res.* **2005**, *41*. [[CrossRef](#)]
50. Lawrence, I.; Lin, K. A concordance correlation coefficient to evaluate reproducibility. *Biometrics* **1989**, 255–268.
51. Huang, H.Q. Reformulation of the bed load equation of Meyer-Peter and Müller in light of the linearity theory for alluvial channel flow. *Water Resour. Res.* **2010**, *46*. [[CrossRef](#)]
52. Huang, H.Q.; Nanson, G.C. Vegetation and channel variation; a case study of four small streams in southeastern Australia. *Geomorphology* **1997**, *18*, 237–249. [[CrossRef](#)]



© 2018 by the authors. Licensee MDPI, Basel, Switzerland. This article is an open access article distributed under the terms and conditions of the Creative Commons Attribution (CC BY) license (<http://creativecommons.org/licenses/by/4.0/>).